JOSA COMMUNICATIONS

The JOSA Communications section is for short papers reporting new results that are deemed to be especially significant or of wide interest. A Communication must be no longer than four printed pages, including title and abstract. Page proofs are provided to authors.

Efficient time-to-space conversion of femtosecond optical pulses

Ayman M. Kan'an and A. M. Weiner

School of Electrical and Computer Engineering, Purdue University, West Lafayette, Indiana 47907-1285

Received August 15, 1997

We report femtosecond time-to-space transformation by means of a potassium niobate nonlinear optical crystal inside a femtosecond pulse shaper. We achieve an upconversion efficiency higher than 50%, a more than 500-fold increase as compared with previous results. We also present theoretical guidelines for estimating the efficiency of such time-to-space converters. © 1998 Optical Society of America [S0740-3224(98)01603-8]

OCIS codes: 320.7110, 320.7100, 320.7160, 070.2580, 190.4410.

1. INTRODUCTION

In recent years powerful techniques for femtosecond waveform synthesis and processing have been demonstrated based on spatial filtering of optical frequency components spectrally dispersed within a femtosecond pulse shaper.[1,2] In essence these techniques transform a one-dimensional parallel optical pattern into a serial signal in the ultrafast time domain. Several groups have also reported the converse—namely, all-optical time-to-space (or serial-to-parallel) transformation of femtosecond optical pulses by spectral holography.[3,4] However, one key problem associated with this approach is slow response (microseconds at best). A related technique for time-to-space conversion of picosecond pulses uses the excitonic optical nonlinearity in ZnSe film material.[5] Although this material has the advantage of fast response time (~13 ps), its operation wavelength is 442 nm, and it has to be cooled to cryogenic temperatures. A third scheme, proposed by Mazurenko, Fainman, and coworkers,[6,7] relies on the instantaneous nonlinear effect of sum frequency mixing (SFM) by means of a nonlinear optical crystal within a pulse shaper. This scheme is an important advance because of the combination of fast response and operation at convenient wavelengths and temperatures. However, in previous short-pulse experiments in which angle-tuned type-I phase matching is used in an LBO crystal,[7] the conversion efficiency was rather low (~0.1%). In the present paper we report achieving femtosecond optical time-to-space mapping with a greater than 50% conversion efficiency by use of temperature-tuned noncritical phase matching (NCPM) in a thick potassium niobate ($KNbO_3$) nonlinear crystal (NLC). This increase in efficiency by more than 500-fold may enable systems using time-to-space mapping in conjunction with smart-pixel optoelectronic-device arrays to perform sophisticated ultrafast pulse-processing operations repeatable at communication rates.

2. EXPERIMENTS

The experimental arrangement, which is similar to that in Ref. 7, is shown in Fig. 1. A short pulse (~125 fs wide) emitted by a mode-locked Ti-sapphire oscillator is split into two beams, a featureless reference pulse $e_r(t)$ and a signal beam $e_s(t)$, which can be shaped. The two beams are diffracted by the single diffraction grating (600 lines/mm) such that the +1 diffraction order from one beam is parallel to the −1 order from the other. The two diffracted beams pass through lens L_1 (with focal length $f_1 = 6$ cm) and are spectrally dispersed in the back Fourier plane of the lens. We have utilized both a collinear as well as a noncollinear geometry, in which the two beams are displaced vertically by a few millimeters at the grating. The two beams interact in the $KNbO_3$ NLC, which is mounted on a thermoelectric cooler for precise temperature control. Since the dispersions of the two beams are equal in amplitude and opposite in sign, the high-frequency components of the signal beam spatially overlap and mix with the low-frequency components of the reference beam, and vice versa. This interaction in a nonlinear crystal, while satisfying the phase-matching condition, results in generating a blue SFM beam that oscillates at the optical frequency $\omega_{SUM} = 2\omega_c$ and is quasi-monochromatic, where ω_c is the center frequency of the input pulses. For a sufficiently short reference pulse, the spatial profile of the blue beam at the output of the NLC is proportional to the Fourier transform of $e_s(t)$. By performing a spatial Fourier transform with lens L_2 (with focal length $f_2 = 16$ cm), a spatial replica of $e_s(t)$ is obtained and recorded with a CCD camera.

Our experiments are performed using a 5 mm × 3 mm × 6.2 mm a-cut $KNbO_3$ crystal. $KNbO_3$ is known to possess a high nonlinear coefficient[8] ($d_{32} \sim 20$ pm/V) and a large damage threshold,[9] and to allow noncritical type-I phase matching for blue generation at ~430 nm by temperature tuning. These properties make this crystal an

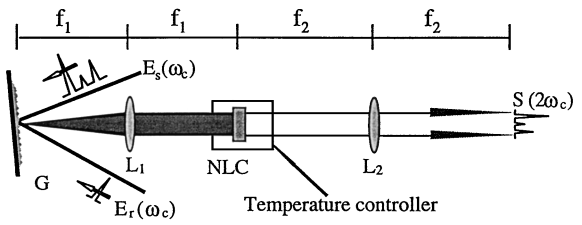

Fig. 1. Schematic of the experimental setup for time-to-space conversion. G, 600 lines/mm diffraction grating; L_1, L_2, Fourier transform lenses; E_s, signal beam; E_r, reference beam; NLC, $KNbO_3$ nonlinear crystal.

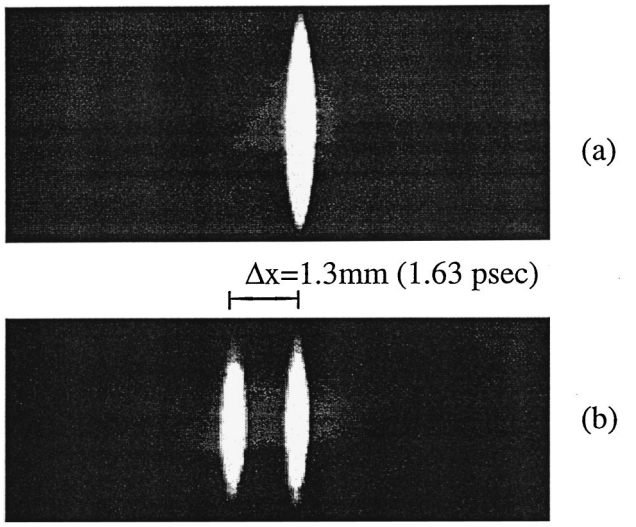

Fig. 2. Images of the SFM blue beams for the interaction of (a) two identical pulses, and (b) one short pulse with two time-delayed signal pulses.

attractive choice for our application. Because of its large group-velocity mismatch (~1.2 ps/mm for 860 to 430 nm conversion) and narrow phase-matching bandwidth (~0.7 nm for crystal length of 6.2 mm), this NLC has been useful only for doubling cw and, to some extent, picosecond pulsed lasers.[10,11] Since our experiment converts femtosecond input pulses into quasimonochromatic upconverted pulses, the narrow phase-matching bandwidth is not a major issue. This permits the use of the large nonlinear coefficient in a NCPM geometry with no spatial walkoff to allow high-conversion efficiency and is an important contribution in our work. In our experiments the fundamental beam propagates along the crystallographic axis a with its polarization along the b axis, generating a nonlinear polarization with a second-harmonic beam polarized along the c axis. In this case the fundamental wavelength can be tuned between 840 nm and 940 nm for temperatures between −38 °C and 180 °C.[12] Here we tune the center wavelength λ_c of the laser to 857.7 nm, which allows type-I NCPM for the quasimonochromatic output at 428.85 nm at room temperature.

Shown in Fig. 2 are the images, in the detector plane, of the blue beam in two cases as the Fourier transforms of the signal and the reference pulses interact in the crystal. In Fig. 2(a) the image shown is for the interaction of two identical pulses with zero time delay between them. On the other hand, Fig. 2(b) shows the image in the case of two signal pulses generated by insertion of a thin glass slide into part of the signal beam. The time-to-space process converts the pulse doublet into two blue spots. Each one of the blue spots is a result of the interaction of one signal pulse and the reference pulse. To demonstrate the linearity of the time-to-space mapping, Fig. 3 shows the displacement of the center of the blue beam in the detection plane as the time delay between the signal and the reference is varied. The calibration constant is estimated to be 0.80 mm/ps, and it is in good agreement with the value 0.776 mm/ps calculated from the expression

$$\frac{\Delta x}{\Delta t} = \frac{f_2 c d \cos\theta_d}{f_1 \lambda_c}\left(\frac{\lambda_{\mathrm{SUM}}}{\lambda_c}\right) = \frac{f_2 c d \cos\theta_d}{2 f_1 \lambda_c}, \qquad (1)$$

where λ_{SUM} is the wavelength of the SFM beam. It is interesting to find that, except for the difference in the ratio $\lambda_{\mathrm{SUM}}/\lambda_c$, this expression is the same as that derived for the case of time-to-space transformation using thin photorefractive material.[3] We should note that in Fig. 2(b), the distance between the two spots was measured to be ~1.3 mm, corresponding to a 1.63-ps time delay. This is in excellent agreement with the predicted value of $\tau = (n-1)s/c = 1.667$ ps, where c is the speed of light, $s = 1$ mm is the thickness of the glass slide inserted into the input of the signal beam to generate the pulse doublet, and $n = 1.5$ is its refractive index.

Also shown in Fig. 3 is the intensity of the SFM beam as the signal pulse is delayed with respect to the reference. This measurement shows that the time window, within which the SFM beam intensity remains at ⩾50% of the peak intensity obtained at zero delay, is $T = 3.9$ ps. The finite time window arises because of the finite spot sizes of individual frequency components focused at the Fourier plane, which limits the spectral resolution of the optical system. An expression for the resulting window has been derived in the context of pulse shaping[2,13] and is given by

$$T = \frac{2\sqrt{\ln 2}\, w_{\mathrm{in}} \lambda_c}{c d \cos\theta_{\mathrm{in}}}. \qquad (2)$$

Here $w_{\mathrm{in}} = 1.05$ mm is the measured radius of the input beam, d is the periodicity of the grating, and $\theta_{\mathrm{in}} = 33°$ is the angle of incidence. Using these values in Eq. (2) we

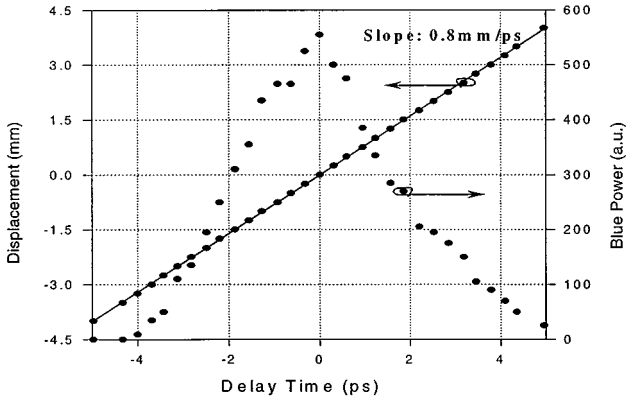

Fig. 3. Variation of the blue power and the displacement of the blue spots as the time delay between the signal and the reference pulses is changed.

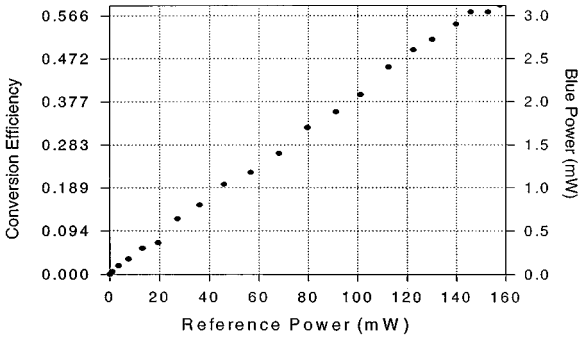

Fig. 4. Variation of the conversion efficiency as a function of the average power of the reference pulse.

obtain $T = 3.66$ ps, in excellent agreement with the data. If desired, the time window can be increased by use of a larger groove density or by an increase of the spot size of the beam at the grating.

The IR signal-to-blue conversion efficiency of this system was measured with a power meter placed close to the output facet of the crystal. The conversion efficiency of the signal beam is expected to depend linearly on the pump power. Shown in Fig. 4 is the variation of the efficiency as the average power of the reference (or pump) beam is varied for a fixed signal average power of 5.3 mW. A linear dependence is observed. At a pump power of 160 mW, 3.12 mW of blue is detected, corresponding to a conversion efficiency of 58%. The data presented in Fig. 4 were obtained with the signal and the reference beams aligned to propagate collinearly in the crystal. This means there is some cross-talk because of the blue light generated by the reference and signal beams individually. Such cross talk due to the individual beam contributions are neglected since (a) only a narrow range of input frequencies very close to ω_c are phase matched, and (b) the blue light generated from the individual beams is spread uniformly over the entire "time window" in the plane of the CCD. Nevertheless, we have also performed experiments in a noncollinear geometry that eliminates the signal from individual beams. In that case we measured a conversion efficiency ~2/3 as large as in Fig. 4. In addition we have measured conversion efficiency versus temperature and found a FWHM temperature tuning range of 1.03 °C for fixed input center wavelength. This is in good agreement with our calculations, which are not described here.

3. CONVERSION EFFICIENCY ANALYSIS

We now estimate the efficiency expected in such time-to-space conversion experiments and discuss the key parameters important for optimizing the efficiency. For nonlinear frequency mixing with Gaussian beams in which a signal beam at ω_s and a reference beam at ω_r generate a SFM beam at ω_{SUM} ($=\omega_s + \omega_r$), the power conversion efficiency η is given by[14]

$$\eta = \frac{P_{\mathrm{SUM}}}{P_s} = \frac{\omega_{\mathrm{SUM}}}{2\omega_s}\sin^2(\Gamma L_{\mathrm{eff}}) \approx \sin^2(\Gamma L_{\mathrm{eff}}), \quad (3)$$

where

$$\Gamma = \left(\frac{2\omega_s\omega_{\mathrm{SUM}}d_{\mathrm{eff}}^2 I_r}{n_s n_r n_{\mathrm{SUM}} c^3 \epsilon_0}\right)^{1/2}. \quad (4)$$

Here P_s, I_r, and P_{SUM} and n_s, n_r, and n_{SUM} are the intensities, powers, and refractive indices associated with the signal, the reference, and the SFM beams, respectively; d_{eff} is the effective nonlinear coefficient, L_{eff} is the effective interaction length in the crystal, and a nondepleted reference beam is assumed. In our experiment the optical frequency components of each input beam are spectrally dispersed at the NLC. The degree of spectral dispersion can be characterized by a parameter N, which is proportional to the ratio of the spatial extent of the dispersed beam to the beam radius w_0 of an individual frequency focused at the nonlinear crystal.[2] At any given spot in the NLC the pulse is stretched in time to a duration $T = Nt_p$, where t_p is the input pulse duration and T is the time window of the system. Both t_p and T refer to the intensity full width at half-maximum. The beam radius w_0 is related to the input beam size, w_{in} by

$$w_0 = \frac{f_1\lambda_c \cos\theta_{\mathrm{in}}}{\pi w_{\mathrm{in}} \cos\theta_d}. \quad (5)$$

Since the reference pulse with energy U_r is dispersed over an area of roughly $N\pi w_0^2/(2\sqrt{2})$ at the NLC (see Appendix A), the reference intensity I_r in Eq. (4) can be written approximately as

$$I_r = \left(\frac{2\sqrt{2}U_r}{\pi w_0^2 N^2 t_p}\right) = \frac{2\sqrt{2}U_r t_p}{\pi w_0^2 T^2}, \quad (6)$$

and therefore

$$\Gamma L_{\mathrm{eff}} = \left(\frac{4\sqrt{2}\omega_s\omega_{\mathrm{SUM}}d_{\mathrm{eff}}^2 U_r t_p L_{\mathrm{eff}}^2}{n^3 c^3 \epsilon_0 \pi w_0^2 T^2}\right)^{1/2}, \quad (7)$$

where we have set $n = n_r \approx n_s \approx n_{\mathrm{SUM}}$.

It is well known that, in the absence of spatial and temporal walkoff, optimum focusing is achieved for $L \approx 2.84b$,[14] where $b = 2\pi n w_0^2/\lambda_c$ is the depth of focus and L is the actual crystal length (6.2 mm). This condition is approximately satisfied in our experiment. The effective interaction length L_{eff} is determined by the minimum of the crystal length L and the depth of focus b. Substituting $L_{\mathrm{eff}} = b$ into Eqs. (3) and (7), one obtains

$$\eta = \sin^2(\Gamma L_{\mathrm{eff}}) = \sin^2\left[\left(\frac{90.5\pi^2 d_{\mathrm{eff}}^2 U_r t_p b}{n^2 c \lambda_c^3 \epsilon_0 T^2}\right)^{1/2}\right]. \quad (8)$$

Substituting in the parameters of our experiment ($U_r = 2$ nJ, $t_p = 125$ fs, $b = 2.8$ mm, $n = 2.278$, and $T = 3.9$ ps), we predict $\Gamma L_{\mathrm{eff}} \approx 0.44\pi$ and $\eta \approx 96\%$. Given the approximate nature of our theoretical treatment, this is in reasonable agreement with our data. This agreement validates our theoretical approach for approximating the conversion efficiency of this time-to-space conversion scheme.

4. DISCUSSION AND SUMMARY

To identify a figure of merit for time-to-space conversion, we consider how the conversion efficiency can be opti-

mized for fixed U_r, t_p, T, and λ_c, since we assume that these parameters will be determined by the system requirements. Clearly one wishes to maximize the quantity $d_{\text{eff}}^2 L/n^2$ while maintaining the optimum focusing condition. One can achieve the desired time window T at the same time as optimum focusing by adjusting both the input beam size and the focal length f_1. Clearly we desire a material that has a large nonlinear coefficient (d_{eff}/n) and that permits noncritical phase matching, which eliminates spatial walkoff to allow for long interaction length. Potassium niobate is an excellent example of such a material for the wavelength range considered here. For high-speed fiber applications in which $\lambda_c \approx 1.55\ \mu$m, periodically poled lithium niobate[15] would be an attractive nonlinear material for similar reasons.

In conclusion, we have presented an efficient, ultrafast time-to-space transformation system using the effect of SFM inside a femtosecond optical-pulse shaper. Efficiency of more than 50% is achieved with type-I noncritical phase matching in a thick $KNbO_3$ nonlinear crystal. This high efficiency may permit the construction of systems with time-to-space conversion used to perform ultrafast pulse processing in real time at frame rates compatible with high-speed communications.

APPENDIX A

The spatial dependence of the reference intensity at the nonlinear crystal can be written in the form

$$|E_r|^2 \sim \exp(-2x^2/w_{\text{eff}}^2)\exp(-2y^2/w_0^2), \tag{A1}$$

where x is the direction of spatial dispersion, y is the other transverse direction, and w_{eff} is an effective beam radius, which accounts for the spatial dispersion. We can relate w_{eff} to the full width at half-maximum bandwidth of the power spectrum (B) by

$$\sqrt{2 \ln 2}\, w_{\text{eff}} = \left|\frac{\partial x}{\partial \nu}\right| B = \frac{\lambda^2 f_1}{cd \cos \theta_d} B. \tag{A2}$$

Here ν is the optical frequency and $\partial x/\partial \nu$ is the spatial dispersion. For Gaussian pulses, the time–bandwidth product is given by

$$Bt_p = \frac{2 \ln 2}{\pi} \approx 0.44. \tag{A3}$$

Using Eq. (A3) and the definition $T = Nt_p$, we can substitute into Eq. (A2) with the result that

$$w_{\text{eff}} = \frac{\sqrt{2 \ln 2}}{\pi} \frac{\lambda^2 f_1}{cd \cos \theta_d} \frac{N}{T}. \tag{A4}$$

Now using Eqs. (2) and (5), we can eliminate T in favor of w_0, as follows:

$$w_{\text{eff}} = \frac{w_0 N}{\sqrt{2}}. \tag{A5}$$

From Eq. (A1), the effective area A_{eff} is given by

$$A_{\text{eff}} = \frac{\pi}{2} w_0 w_{\text{eff}}, \tag{A6}$$

where we define effective area by the requirement that an elliptical beam with area A_{eff} and constant intensity equal to the actual on-axis intensity have the same power as the actual Gaussian beam. From Eq. (A5), the result is

$$A_{\text{eff}} = \frac{N \pi w_0^2}{2\sqrt{2}}. \tag{A7}$$

ACKNOWLEDGMENT

The authors gratefully acknowledge support from the U.S. Department of Defense Focused Research Initiative, U.S. Air Force Office of Scientific Research grant F49620-95-1-0533.

REFERENCES

1. A. M. Weiner, J. P. Heritage, and E. M. Kirschner, J. Opt. Soc. Am. B **5**, 1563 (1988).
2. A. M. Weiner, Prog. Quantum Electron. **19**, 161 (1995), and the references cited therein.
3. M. C. Nuss, M. Li, T. H. Chiu, A. M. Weiner, and A. Partovi, Opt. Lett. **19**, 664 (1994).
4. P. C. Sun, Y. T. Mazurenko, W. S. C. Chang, P. L. Yu, and Y. Fainman, Opt. Lett. **20**, 1728 (1995).
5. K. Ema, M. Kuwata-Gonokami, and F. Shimizu, Appl. Phys. Lett. **59**, 2799 (1991).
6. Y. T. Mazurenko, S. E. Putilin, A. G. Spiro, A. G. Beliaev, V. E. Yashin, and S. A. Chizhov, Opt. Lett. **21**, 1753 (1996).
7. P. C. Sun, Y. T. Mazurenko, and Y. Fainman, J. Opt. Soc. Am. A **14**, 1159 (1997).
8. See, for example, J.-C. Baumert and P. Günter, Appl. Phys. Lett. **50**, 554 (1987).
9. U. Ellenberger, R. Weber, J. E. Balmer, B. Zysset, D. Ellgehausen, and G. Mizell, Appl. Opt. **31**, 7563 (1992).
10. Y. Lu, Q. Zhao, Y. Li, H. He, Q. Zou, Z. Lu, and Z. Gang, Opt. Lett. **32**, 713 (1993).
11. E. S. Polzik and H. G. Kimble, Opt. Lett. **16**, 1400 (1991).
12. I. Biaggio, P. Kerkoc, L. S. Wu, P. Günter, and B. Zyssett, J. Opt. Soc. Am. B **9**, 507 (1992).
13. R. N. Thurston, J. P. Heritage, A. M. Weiner, and W. J. Tomlinson, IEEE J. Quantum Electron. **22**, 682 (1986).
14. See, for example, *Nonlinear Optics*, P. G. Harper and B. S. Wherrett, eds. (Academic, New York, 1977).
15. M. M. Fejer, G. A. Magel, D. H. Jundt, and R. Beyer, IEEE J. Quantum Electron. **28**, 2631 (1992).